Acta Crystallographica Section D
Biological Crystallography
ISSN 0907-4449

The structure of human deoxycytidine kinase in complex with clofarabine reveals key interactions for prodrug activation

Yan Zhang,[a] John A. Secrist III[b] and Steven E. Ealick[c]*

[a]Department of Molecular Biology and Genetics, Cornell University, Ithaca, NY 14853, USA, [b]Drug Discovery Division, Southern Research Institute, Birmingham, AL 35205, USA, and [c]Department of Chemistry and Chemical Biology, Cornell University, Ithaca, NY 14853, USA

Correspondence e-mail: see3@cornell.edu

Received 16 August 2005
Accepted 21 October 2005

PDB Reference: dCK–clofarabine–ADP, 2a7q, r2a7qsf.

Clofarabine [2-chloro-9-(2-deoxy-2-fluoro-β-D-arabinofuranosyl)-9*H*-purin-6-amine] is a hybrid of the widely used anticancer drugs cladribine and fludarabine. It is the precursor of an effective chemotherapeutic agent for leukemias and other hematological malignancies and received accelerated approval by the FDA for the treatment of pediatric patients with relapsed or refractory acute lymphoblastic leukemia. Clofarabine is phosphorylated intracellularly by human deoxycytidine kinase (dCK) to the 5′-monophosphate, which is the rate-limiting step in activation of the prodrug. dCK has a broad substrate specificity, with a much higher activity to deoxycytidine than to deoxyadenosine and deoxyguanosine. As a purine-nucleoside analog, clofarabine is a better substrate of dCK than deoxycytidine. The crystal structure of dCK has been solved previously in complex with pyrimidine nucleosides and ADP [Sabini *et al.* (2003), *Nature Struct. Biol.* **10**, 513–519]. In the current study, the crystal structure of clofarabine- and ADP-bound dCK was solved to 2.55 Å by molecular replacement. It appears that the enzyme takes the same conformation as in the structures of the pyrimidine nucleoside-bound complexes. The interactions between 2-Cl and its surrounding hydrophobic residues contribute to the high catalytic efficiency of dCK for clofarabine.

1. Introduction

Anticancer chemotherapy has long been an attractive research field and nucleoside analogs are among the anticancer chemotherapeutic agents that have drawn intense attention from both basic researchers and clinical scientists (Elion, 1989; Heidelberger *et al.*, 1983). Nucleoside analogs target nucleotide metabolism in rapidly proliferating neoplastic cells mainly by either blocking DNA synthesis (Cheng *et al.*, 1981; Mikita & Beardsley, 1988) or by interfering with the recycling of the cellular nucleotide pool (Kanazawa *et al.*, 1998). The purine-nucleoside analogs cladribine (2-chlorodeoxyadenosine) and fludarabine (9-β-D-arabinofuranosyl-2-fluoroadenine 5′-monophosphate) have been widely used in the treatment of hematological malignancies (Avramis & Plunkett, 1982; Beutler & Carson, 1993; Brockman *et al.*, 1980; Keating *et al.*, 1998; Piro *et al.*, 1988; Santana *et al.*, 1992; Warrell & Berman, 1986). Cladribine carries out anticancer activity primarily by inhibiting ribonucleotide reductase (RNR), thereby decreasing cellular deoxynucleoside triphosphate pools (Griffig *et al.*, 1989). However, the oral bioactivity of cladribine is hampered (Liliemark *et al.*, 1992) by instability at low pH (Carson *et al.*, 1992; Reichelova *et al.*, 1995) and rapid glycosidic bond cleavage by bacterial purine-nucleoside phosphorylase (PNP; Bzowska & Kazimierczuk, 1995). Fludarabine-induced cytotoxicity is mainly by inhibition of

DNA polymerase (Huang *et al.*, 1990). Despite its excellent antitumor activity, fludarabine has severe neurotoxicity at high dosage (Warrell & Berman, 1986), possibly owing to 2-fluoroadenine, a phosphorolytic cleavage product of *Escherichia coli* PNP (Huang & Plunkett, 1987; Struck *et al.*, 1982).

To improve the efficacy, minimize the toxicity and increase the stability, a rationally designed hybrid of cladribine and fludarabine, clofarabine [2-chloro-9-(2-deoxy-2-fluoro-β-D-arabinofuranosyl)-9*H*-purin-6-amine] (Fig. 1*a*), was synthesized (Montgomery *et al.*, 1992). Clofarabine incorporates the favorable properties but overcomes most of the drawbacks of cladribine and fludarabine. Clofarabine triphosphate, the active form of clofarabine, terminates DNA elongation (Parker *et al.*, 1991) and impacts DNA repair (Yamauchi *et al.*, 2001) by inhibition of DNA polymerase after incorporation into the DNA chain (Xie & Plunkett, 1995). Depletion of deoxynucleotide pools by inhibition of RNR is another primary mechanism of the inhibition of DNA synthesis by clofarabine triphosphate (Parker *et al.*, 1991; Xie & Plunkett, 1996). In addition, clofarabine induces DNA fragmentation and apoptosis (Carson *et al.*, 1992) by interfering with mitochondrial integrity (Genini *et al.*, 2000). Therefore, clofarabine is cytotoxic not only to rapidly proliferating cancer cells but also to non-dividing quiescent cancer cells. With the halogenation at the 2-position of adenine, clofarabine is resistant to deamination by adenosine deaminase. Substitution of a fluorine at the 2′-carbon in the *arabino* configuration makes clofarabine highly resistant to phosphorolysis by bacterial PNP and increases the stability of clofarabine at acidic pH (Carson *et al.*, 1992; Reichelova *et al.*, 1995). The excellent performance of clofarabine in biochemical and pharmacological trials led to clinical trials (Faderl *et al.*, 2005; Jeha *et al.*, 2004; Kantarjian *et al.*, 2003; Pui *et al.*, 2005). In December 2004, clofarabine was approved by the US Food and Drug Administration under its accelerated approval process for the treatment of pediatric patients 1–21 y old with relapsed or refractory acute lymphoblastic leukemia after at least two prior regimens (FDA labelling information). It is the first new drug for pediatric leukemia to be approved in more than a decade. To exhibit cytotoxic activity, clofarabine must be phosphorylated to clofarabine triphosphate. During this process, the initial phosphorylation to the monophosphate by deoxycytidine kinase (dCK) is the rate-limiting step and plays a crucial role in the activation of the prodrug (Lotfi *et al.*, 1999; Parker *et al.*, 1991).

Human dCK is a homodimer with 260 residues per subunit. It can phosphorylate the pyrimidine nucleoside deoxycytidine (dC) and the purine nucleosides deoxyadenosine (dA) and deoxyguanosine (dG), with a much higher activity for dC (Bohman & Eriksson, 1988; Datta *et al.*, 1989). dCK phosphorylates clofarabine with a 50% lower K_M but a fourfold higher V_{max} than the physiological substrate dC (Lotfi *et al.*, 1999). The crystal structure of human dCK has previously been solved in complex with ADP and various pyrimidine nucleosides, including the natural substrate dC and the prodrugs cytarabine (1-β-D-arabinosylcytosine) and gemcitabine (2′,2′-difluorodeoxycytidine) (Sabini *et al.*, 2003). The structure suggests that Arg128 plays an important role in the efficacy of pyrimidine-nucleoside prodrugs as substrates. Notably, dCK shares 47% sequence identity with human mitochondrial deoxyguanosine kinase (dGK), which has specific activity toward purine nucleosides (Wang *et al.*, 1993, 1996). Clofarabine is also a good substrate of dGK (Sjöberg *et al.*, 1998), which may contribute to its role in mitochondrial damage (Genini *et al.*, 2000). The structure of human dGK, in which an ATP molecule was unexpectedly bound to the dG-binding site, has previously been determined (Johansson *et al.*, 2001).

To gain additional insight into the structure–activity relationships of purine-nucleoside analogs as prodrugs, we have determined the crystal structure of human dCK in complex with the purine-nucleoside analog clofarabine and ADP. A comparison of this structure with other structures of dCK in complex with pyrimidine-nucleoside analogs (Sabini *et al.*, 2003) reveals the key interactions that contribute to the high catalytic efficiency for clofarabine. This study provides a structural basis for developing more effective drugs and for protein engineering in the application of prodrug activation *via* gene therapy.

2. Experimental procedures

2.1. Gene cloning and expression

The human *dck* gene was PCR-amplified in two parts from pDCK.3d using the following primer pairs: upstream primer 5′-tag tag cat ATG GCC ACC CCG CCC AAG AGA AGC-3′ (inserts an *Nde*I site at the start codon of the *dck* open reading frame), downstream primer 5′-CGA CTG AGA CAG GCA TAA GTT TGG AAG GTA AAA GAC-3′ (removes an internal *Nde*I) and upstream primer 5′-GTC TTT TAC CTT CCA AAC TTA TGC CTG TCT CAG TCG-3′ (removes an

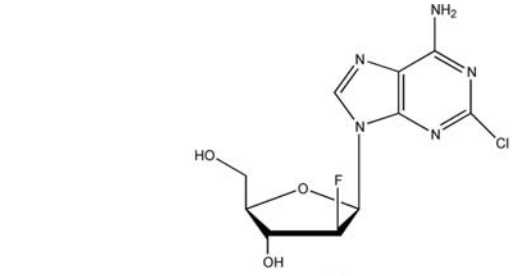

(*a*)

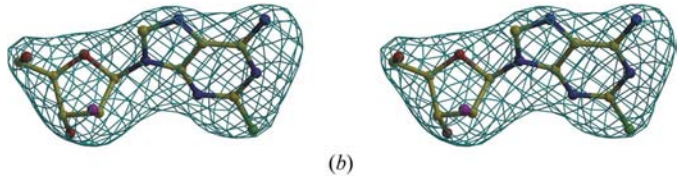

(*b*)

Figure 1
Clofarabine. (*a*) The structure of clofarabine. (*b*) Electron density of clofarabine. The $F_o - F_c$ omit map was calculated to 2.55 Å after one cycle of refinement without clofarabine from the model (blue–green mesh, contoured at 3σ). Clofarabine is drawn in ball-and-stick representation.

internal *Nde*I site) and the T7 terminator primer as the downstream primer. The two PCR products were mixed and PCR was repeated with the outmost two primers to give an amplified product containing *dck* with an internal *Nde*I site removed and an *Nde*I site inserted at the start codon. The amplified product also contained a small amount of vector-derived DNA after the *dck* stop codon. The purified PCR product was ligated into pCR4Blunt-TOPO using the Zero Blunt TOPO PCR Cloning kit for Sequencing from Invitrogen (Carlsbad, CA, USA). Colonies were screened for presence of the insert and a representative plasmid was designated pDCK.TOPO. The PCR-derived DNA was sequenced and shown to contain no errors. The *dck* gene was excised from pDCK.TOPO by digestion with *Nde*I and *Bam*HI and ligated into similarly digested pET-28a to give the overexpression plasmid pDCK.28.

The plasmid pDCK.28 was transformed into *E. coli* strain BL21(DE3) (Novagen). The transformed cells were grown in 20 ml of LB containing 50 µg ml^{-1} kanamycin at 310 K until the OD_{600} reached 0.8. This culture was inoculated into 1 l 2YT medium containing the same antibiotic. The resulting culture was grown at 310 K until the OD_{600} reached 0.6. Expression was induced by addition of isopropyl β-D-thio-galactopyranoside to a final concentration of 0.1 m*M*. The cells were harvested after 6 h by centrifugation at 3000*g* for 20 min at 277 K and were stored at 193 K.

2.2. Protein purification

All purification steps were carried out at 277 K. Cells were resuspended in a tenfold excess (*w*/*v*) of lysis buffer containing 50 m*M* sodium phosphate and 300 m*M* sodium chloride pH 8.0 and lysed by sonication. The crude extract was centrifuged at 12 000*g* for 25 min and the supernatant was loaded onto a Talon IMAC resin (BD) column pre-equilibrated with lysis buffer. After washing the column with wash buffer containing 50 m*M* sodium phosphate, 300 m*M* sodium chloride, 10 m*M* imidazole pH 7.0, the protein was eluted from the resin with elution buffer containing 50 m*M* sodium phosphate, 300 m*M* sodium chloride, 300 m*M* imidazole pH 7.0 and the His tag was removed using thrombin. The protein was further purified on a MonoQ HR 10/10 Pharmacia column and a G75 Pharmacia gel-filtration column. The protein was buffer-exchanged into 20 m*M* Tris, 10 m*M* $MgCl_2$, 5 m*M* dithiothreitol pH 7.0 using an Econo-Pac 10DG column (Bio-Rad) and then concentrated to 15 mg ml^{-1} using a 10 kDa cutoff concentrator (Amicon). The purity of dCK was determined by Coomassie-stained SDS–PAGE and found to be greater than 95% (data not shown). The purified protein was stored at 193 K until needed.

2.3. Crystallization of dCK

The dCK–clofarabine–ADP complex was crystallized at 295 K using the hanging-drop vapor-diffusion method. Each drop contained 1 µl protein solution and 1 µl reservoir solution. The protein solution contained 12 mg ml^{-1} dCK, 4 m*M* clofarabine and 4 m*M* ADP. The reservoir solution for the optimized conditions contained 0.9 *M* sodium citrate, 0.1 *M* HEPES pH 7.0. Crystals grew over 7 d to their maximum size (0.15 × 0.15 × 0.1 mm). The crystals belong to the tetragonal space group $P4_32_12$, with unit-cell parameters a = 80.15, b = 80.15, c = 93.67 Å. This corresponds to a solvent content of 53% with one monomer per asymmetric unit.

Table 1
Data-collection and refinement statistics.

Values for the outer resolution shell are given in parentheses.

Data collection	
Wavelength (Å)	0.9790
Resolution (Å)	2.55
Space group	$P4_32_12$
Unit-cell parameters	
a (Å)	80.15
b (Å)	80.15
c (Å)	93.67
No. of reflections	61609
No. of unique reflections	9726
Redundancy	6.3 (4.6)
Completeness (%)	92.3 (54.6)
R_{sym}† (%)	4.9 (16.1)
$I/\sigma(I)$	35.2 (6.4)
Refinement	
Total No. of non-H atoms	1972
No. of protein atoms	1875
No. of ligand atoms	48
No. of water O atoms	49
No. of reflections in refinement	9237
No. of reflections in test set	755
R factor‡ (%)	21.3
R_{free}§ (%)	24.6
R.m.s. deviation from ideal geometry	
Bonds (Å)	0.009
Angles (°)	1.3
Ramachandran plot	
Most favored region (%)	89.5
Additionally allowed region (%)	10.0
Generously allowed region (%)	0
Disallowed region (%)	0.5

† $R_{sym} = \sum\sum_i |I_i - \langle I\rangle| / \sum\langle I\rangle$, where $\langle I\rangle$ is the mean intensity of N reflections with intensities I_i and common indices h, k and l. ‡ R factor = $\sum_{hkl} \big||F_{obs}| - k|F_{calc}|\big| / \sum_{hkl} |F_{obs}|$, where F_{obs} and F_{calc} are the observed and calculated structure factors, respectively. § For R_{free}, the sum is extended over a subset of reflections (8%) excluded from all stages of refinement.

2.4. X-ray data collection and processing

The data were collected from a flash-frozen crystal at cryogenic temperatures. The crystals were cryoprotected by a quick dip in a mixture of Paratone and paraffin in a 1:2 volume ratio and then flash-frozen in liquid nitrogen. Monochromatic X-ray intensity data were measured at the Advanced Photon Source on the NE-CAT 24-ID beamline using a Quantum-315 CCD detector (Area Detector Systems Corp.). Data were collected at a wavelength of 0.979 Å over a range of 90° using 2 s exposures for each 0.5° oscillation at a crystal-to-detector distance of 350 mm. The *HKL*2000 suite (Otwinowski & Minor, 1997) of programs was used for integration and scaling of data. Details of data collection and processing are given in Table 1.

2.5. Structure determination and model refinement

The structure of the dCK–clofarabine–ADP complex was determined by molecular replacement using the *CNS* software package (Brünger *et al.*, 1998) and the published human dCK structure (PDB code 1p61; Sabini *et al.*, 2003) as the search model. A solution with a correlation coefficient of 0.64 was obtained using the data between 10 and 4 Å resolution. The subsequent refinement, including successive rounds of simulated-annealing refinement, energy minimization and temperature-factor refinement, was performed using *CNS* followed by manual remodeling with the computer-graphics program *O* (Jones *et al.*, 1991). Clofarabine and ADP were well defined in an $F_o - F_c$ electron-density map contoured at 3σ and were manually fitted. Bond-distance and bond-angle restraints for clofarabine were generated using the program *PRODRG* (Schüttelkopf & van Aalten, 2004). The model was examined using *CNS* and *PROCHECK* (Laskowski *et al.*, 1993). The final refinement statistics are summarized in Table 1.

Figures were prepared using *MOLSCRIPT* (Kraulis, 1991), *BOBSCRIPT* (Esnouf, 1999) and *RASTER3D* (Merritt & Murphy, 1994).

3. Results and discussion

3.1. Overall structure

This dCK–clofarabine–ADP complex is the first reported structure of dCK complexed with a purine-nucleoside analog. The final model, refined at 2.55 Å, contains 1876 protein atoms, one clofarabine molecule, one ADP molecule, one magnesium ion and 50 water molecules. Residues 1–19 and 65–76 are disordered and were not included in the final model. The crystallographic *R* factor is 21.3% and R_{free} is 24.5%. The Ramachandran plot shows 89.5% of the residues in the most favorable region, 10.0% in the additionally allowed region and one residue (Arg128) in the disallowed region. Residue Arg128 is located at the active site and is represented by clear electron density. The electron density of clofarabine is shown in Fig. 1(*b*).

In the crystal structure, dCK is a homodimer. The overall fold of each subunit is an $\alpha\beta\alpha$ three-layer sandwich. The central parallel β-sheet contains five strands with topology $\beta2\beta3\beta1\beta4\beta5$ flanked by ten α-helices and a few 3_{10}-helices. The helix containing residues 182–192, the 3_{10}-helix of residues 196–199 and the loop connecting them form a lid that folds back over the substrate-binding site. This structure is essentially the same as the previously described structures of dCK in complex with pyrimidine analogs (Sabini *et al.*, 2003). A comparison of dCK–clofarabine–ADP and other dCK complexes shows a root-mean-square deviation (r.m.s.d.) of 0.4–0.5 Å for the pairwise comparison of the C^{α} atoms of all ordered residues. The overall fold of the dCK complex is also similar to that of human deoxyguanosine kinase (dGK), with an r.m.s.d. of 1.4 Å.

3.2. Deoxynucleoside-binding site

The active site of dCK is located along the C-terminal edge of the central β-sheet and is covered by the lid. Clofarabine is almost completely buried in a pocket inside the enzyme and is shielded from the solvent. The clofarabine molecule assumes a standard *anti* conformation, with a glycosidic torsion angle of -155° (Fig. 1*b*). Similarly to the pyrimidine analogs, the 5′-phydroxyl group of the sugar forms hydrogen bonds with Glu53 O^{ε} and a water molecule. The 3′-hydroxyl group accepts a hydrogen bond from Tyr86 O^{η} and provides a hydrogen bond to Glu197 O^{ε}, which is located at the lid. The 2′-arabinosyl fluorine is close to Lys128 N^{η}, which also makes hydrogen bonds to the side chain of Glu53 and the carbonyl O atom of Gly28. However, both experimental and theoretical studies suggest that a possible hydrogen bond involving the fluorine does not significantly contribute to the overall substrate binding (Dunitz, 2004). Additional interactions between clofarabine and the active site come from the adenine base. The N1 atom forms a hydrogen bond with Gln97 N^{ε}. The

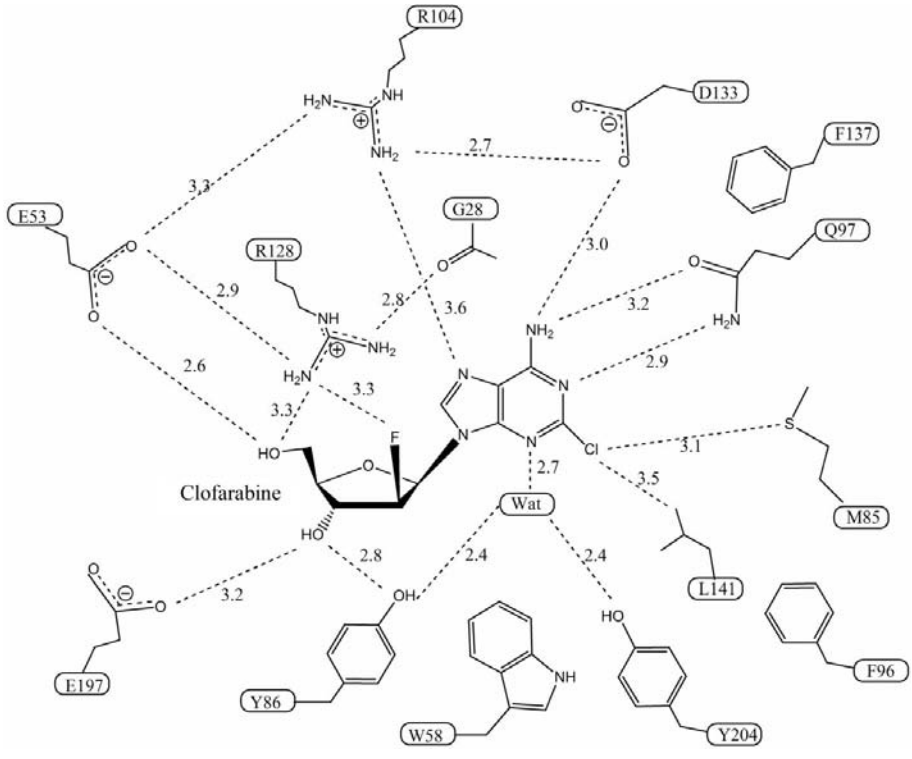

Figure 2
A schematic drawing of the deoxynucleoside-binding site. Key hydrogen bonds and van der Waals interactions are indicated by dashed lines with the corresponding distances in Å labelled.

N6 atom forms bifurcated hydrogen bonds with Asp133 O^{δ} and Gln97 O^{ε}. The N3 atom makes a hydrogen bond with a water molecule that in turn makes hydrogen bonds with Tyr86 and Tyr204. The N7 atom may form a weak hydrogen bond with Arg104 N^{η} with a distance of 3.6 Å. The 2-Cl atom makes van der Waals interactions with Met85 S^{δ} and Leu141 C^{δ}. One face of the adenine ring stacks against the aromatic ring of Phe137 and the other makes close contacts (less than 3.4 Å) with the side chains of Phe96 and Trp58 (Fig. 2).

When the active site of the dCK–clofarabine–ADP complex is superimposed on the active sites of dCK in complex with pyrimidine-nucleoside analogs (Sabini *et al.*, 2003), clofarabine is translated about 1 Å along the glycosidic bond direction toward the sugar (Fig. 3*a*). The main-chain atoms of the enzyme maintain their positions, while the side chains move subtly to maintain the interactions between the substrate and the enzyme. Consequently, N6 of adenine positionally corresponds to N4 of cytosine, N1 corresponds to N3 and N3 corresponds to O2, and their interactions with the enzyme remain the same. The difference at the adenine moiety comes from the N7 and 2-halogenation. The sugar moiety of clofarabine also retains the same hydrogen-bonding network as the pyrimidine-nucleoside analogs. The interaction between the 2′-arabinosyl fluorine and Arg128 is also present in the gemcitabine-bound dCK complex. There has been a controversy over whether dCK employs different conformational states for pyrimidine nucleosides and purine nucleosides (Bohman & Eriksson, 1988; Johnsamuel *et al.*, 2005; Kierdaszuk & Eriksson, 1990; Kierdaszuk *et al.*, 1993). In the current structural study, the active site of purine-nucleoside analog-bound dCK appears to be the same as those of pyrimidine nucleoside-bound dCK. This suggests that the purine nucleosides may bind to dCK in a similar manner to the pyrimidine nucleosides. The different catalytic preferences of the substrates for different bases may arise from the specific interactions of the substrates with the enzyme. Alternatively, clofarabine may mimic dC binding to dCK by a positional shift at the active site induced by the 2-substitution or 2′-halogenation.

Human dCK shares 47% sequence identity with human dGK, with most of the active-site residues conserved. When compared with dGK (Johansson *et al.*, 2001), clofarabine-bound dCK reveals the most pronounced differences at residues Glu53, Arg104 and Asp133, which line one side of the substrate-binding site (Fig. 3*b*). In dGK, an ATP molecule is bound at the nucleoside-binding site, with the adenosine moiety superimposed well on clofarabine. In dGK, Glu70 (corresponding to Glu53 of dCK) flips away from the 5′-O atom and accepts a hydrogen bond from Arg118 N^{ε} (corresponding to Arg104 of dCK). In an extended conformation, Arg118 is anchored by Asp147 (corresponding to Asp133 of dCK), which is in turn stabilized by hydrogen bonds to Ser114 and Tyr169. Clofarabine is as effective as a substrate of dGK as dG (Sjöberg *et al.*, 1998). It is reasonable to assume that clofarabine would bind to dGK in a manner similar to other purine nucleosides. Therefore, almost all the interactions of the adenosine moiety of ATP with the enzyme would be present when clofarabine is bound to dGK. One exception may be Glu70. In ATP-bound dGK, Glu70 points away from the substrate-binding site, most likely owing to steric hindrance from the α-phosphate of ATP. When clofarabine binds, Glu70 O^{ε} may make a hydrogen bond with the 5′-hydroxyl group, serving as a general base as suggested previously (Eriksson *et al.*, 2002; Wild *et al.*, 1997). In addition to the interactions of the adenosine moiety with the enzyme, 2′-F would form a hydrogen bond with Arg142 of dGK (corresponding to Arg128 of dCK).

3.3. ATP-binding site

Attempts to crystallize dCK and clofarabine with an ATP analog were not successful. Instead, ADP was used and was found to be bound at the active site. ADP is positioned in a shallow groove, mostly exposed to the solvent. In contrast to clofarabine, the adenosine moiety of ADP does not make extensive interactions with the enzyme. The N1 and N6 atoms make hydrogen bonds with the amide N atom of Phe242 and the carbonyl O atom of Glu240, respectively. The adenine ring is stacked against the side chain of Arg188. One of the O atoms of the α-phosphate is hydrogen bonded to the hydroxyl group of Thr36. The O atoms of the β-phosphate interact with the amide N atom and the N^{ζ} atom of Lys34, the amide N atom of Ser35 and the Mg^{2+} ion. The Mg^{2+} ion was included based on the presence of 10 m*M* $MgCl_2$ in the protein solution, the coordination geometry and the refined *B* factors. In the cytarabine- and gemcitabine-bound structures (Sabini *et al.*, 2003), an Mg^{2+} ion was also found at the same position, presumably between the β- and γ-phosphates of ATP.

3.4. Structure–activity relationships

Deoxyadenosine (dA) is a poor substrate of dCK (Bohman & Eriksson, 1988). With 2- and 2′-halogenation, clofarabine is an excellent substrate of dCK (Lotfi *et al.*, 1999). The 2-Cl is located in a hydrophobic pocket and makes interactions with Met85 and Leu141 (Figs. 2 and 3). Cladribine, which only differs from dA by a 2-Cl substitution, has a K_M two orders of magnitude lower than dA, but a comparable V_{max} (Bohman & Eriksson, 1988; Datta *et al.*, 1989). The above observations suggest that the interactions between 2-Cl and surrounding hydrophobic residues play an important role in the affinity and catalytic efficiency of dCK. Additional improvement of catalytic efficiency comes from the 2′-arabinosyl fluorine. The 2′-position has crowded surroundings, with Arg128, Leu30 and Tyr86 nearby. When the 2′-arabinosyl position contains hydrogen, one of the N^{η} atoms of Arg128 is able to provide a hydrogen bond to the 5′-hydroxyl and another hydrogen bond to Glu53 at the same time. Glu53 in turn forms a hydrogen bond with the 5′-hydroxyl group and deprotonates it as a general base (Eriksson *et al.*, 2002; Wild *et al.*, 1997). When fluorine is present at the 2′-arabinosyl position, it is close enough to make a hydrogen bond with Arg128. However, fluorine in organic molecules is a poor hydrogen-bond acceptor (Dunitz, 2004). Nevertheless, the rearrangement of Arg128 allows Glu53 to fulfil its role in the deprotonation of

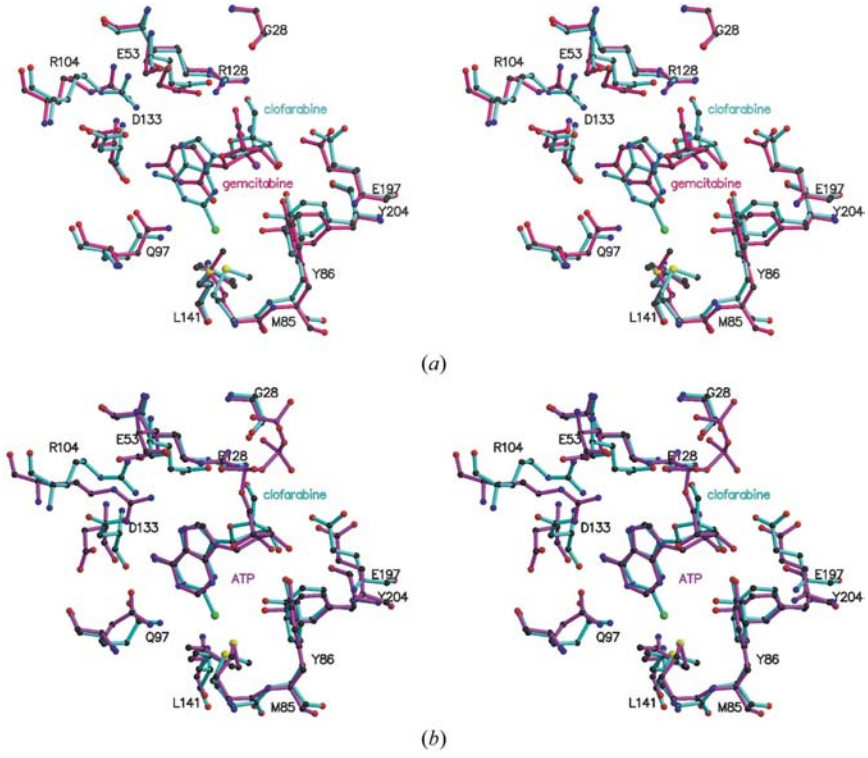

Figure 3
Stereoview of the superposition of the active sites. (*a*) Superposition of clofarabine-bound dCK (cyan) and gemcitabine-bound dCK (pink). (*b*) Superposition of the active sites of clofarabine-bound dCK (cyan) and dGK (magenta). The superposition was based on the C^{α} positions of all ordered residues in the two structures. The residues and nucleosides are shown in ball-and-stick representations. The residues are labelled by their single-letter amino-acid codes and residue numbers.

the 5′-hydroxyl and consequently improves the reaction rate. On the other hand, with a small group at the 2′-ribosyl position the interactions between Tyr86 and Leu30 cannot contribute to the deprotonation of the 5′-hydroxyl, although they may improve the binding of the substrates. This is supported by the observation that clofarabine is a better substrate than either 2-chloro-9-(2-deoxy-2-fluoro-β-D-ribofuranosyl)adenine or 2-chloro-9-(2-deoxy-2,2-difluoro-β-D-ribofuranosyl)adenine (Parker *et al.*, 1999).

The current structural information suggests dCK mutants that might have higher efficiency for the purine-nucleoside prodrugs, which could be used in gene therapy of solid tumors (Sorscher *et al.*, 1994). In clofarabine-bound dCK, Arg104 makes a hydrogen bond with Glu53 and as well as a weak hydrogen bond with the N7 of clofarabine. N7 may compete with the Glu53 interaction with Arg104, consequently contributing to the catalytic efficiency of clofarabine. When the physiological purine nucleosides are bound, the N7–Arg104 interaction may account for the V_{max} of purine nucleosides being fivefold higher than pyrimidine nucleosides, although the affinity of dCK for the former is 100-fold lower than for the latter. Based on the structure of dGK, mutation of Ala100 to Ser may allow Asp133 to adopt another rotamer (Johansson *et al.*, 2001), which may in turn anchor Arg104 in an extended conformation. In turn, Arg104 would make a strong interaction with N7, facilitating the deprotonation of the 5′-hydoxyl by Glu53.

4. Conclusions

The structure of human dCK in complex with clofarabine and ADP is the first example of a purine analog complexed with this important activator of nucleoside-analog prodrugs. The structure reveals that both purine and pyrimidine analogs display similar active-site geometries. The presence of the 2-chloro substituent in clofarabine causes a 1 Å shift of the substrate and is probably responsible for the enhanced catalytic efficiency of dCK for clofarabine. The structure also suggests modifications to dCK that might make it useful as a prodrug activator in the gene-therapy approach to anticancer treatment.

We thank the NE-CAT beamline 24-ID of the Advanced Photon Source, supported by grant RR15301 from the National Council on Research Resources of NIH, for providing beam time for the study. We thank Dr Cynthia Kinsland for the preparation of the His-tagged DCK overexpression plasmid. We thank Dr Angela V. Toms for assistance with data collection and Leslie Kinsland for assistance with the preparation of this manuscript. This work was also supported by NIH grant 2P01CA34200.

References

Avramis, V. I. & Plunkett, W. (1982). *Cancer Res.* **42**, 2587–2591.
Beutler, E. & Carson, D. A. (1993). *Blood Cells*, **19**, 559–572.
Bohman, C. & Eriksson, S. (1988). *Biochemistry*, **27**, 4258–4265.
Brockman, R. W., Cheng, Y. C., Schabel, F. M. Jr & Montgomery, J. A. (1980). *Cancer Res.* **40**, 3610–3615.
Brünger, A. T., Adams, P. D., Clore, G. M., DeLano, W. L., Gros, P., Grosse-Kunstleve, R. W., Jiang, J.-S., Kuszewski, J., Nilges, M., Pannu, N. S., Read, R. J., Rice, L. M., Simonson, T. & Warren, G. L. (1998). *Acta Cryst.* D**54**, 905–921.
Bzowska, A. & Kazimierczuk, Z. (1995). *Eur. J. Biochem.* **233**, 886–890.
Carson, D. A., Wasson, D. B., Esparza, L. M., Carrera, C. J., Kipps, T. J. & Cottam, H. B. (1992). *Proc. Natl Acad. Sci. USA*, **89**, 2970–2974.
Cheng, Y. C., Derse, D., Tan, R. S., Dutschman, G., Bobek, M., Schroeder, A. & Bloch, A. (1981). *Cancer Res.* **41**, 3144–3149.
Datta, N. S., Shewach, D. S., Hurley, M. C., Mitchell, B. S. & Fox, I. H. (1989). *Biochemistry*, **28**, 114–123.
Dunitz, J. D. (2004). *ChemBioChem*, **5**, 614–621.
Elion, G. B. (1989). *Science*, **244**, 41–47.
Eriksson, S., Munch-Petersen, B., Johansson, K. & Eklund, H. (2002). *Cell. Mol. Life Sci.* **59**, 1327–1346.
Esnouf, R. M. (1999). *Acta Cryst.* D**55**, 938–940.
Faderl, S., Gandhi, V., Keating, M. J., Jeha, S., Plunkett, W. & Kantarjian, H. M. (2005). *Cancer*, **103**, 1985–1995.

Genini, D., Adachi, S., Chao, Q., Rose, D. W., Carrera, C. J., Cottam, H. B., Carson, D. A. & Leoni, L. M. (2000). *Blood*, **96**, 3537–3543.
Griffig, J., Koob, R. & Blakley, R. L. (1989). *Cancer Res.* **49**, 6923–6928.
Heidelberger, C., Danenberg, P. V. & Moran, R. G. (1983). *Adv. Enzymol. Relat. Areas Mol. Biol.* **54**, 58–119.
Huang, P., Chubb, S. & Plunkett, W. (1990). *J. Biol. Chem.* **265**, 16617–16625.
Huang, P. & Plunkett, W. (1987). *Biochem. Pharmacol.* **36**, 2945–2950.
Jeha, S., Gandhi, V., Chan, K. W., McDonald, L., Ramirez, I., Madden, R., Rytting, M., Brandt, M., Keating, M., Plunkett, W. & Kantarjian, H. (2004). *Blood*, **103**, 784–789.
Johansson, K., Ramaswamy, S., Ljungcrantz, C., Knecht, W., Piskur, J., Munch-Petersen, B., Eriksson, S. & Eklund, H. (2001). *Nature Struct. Biol.* **8**, 616–620.
Johnsamuel, J., Eriksson, S., Oliveira, M. & Tjarks, W. (2005). *Bioorg. Med. Chem.* **13**, 4160–4167.
Jones, T. A., Zou, J.-Y., Cowan, S. W. & Kjeldgaard, M. (1991). *Acta Cryst.* A**47**, 110–119.
Kanazawa, J., Takahashi, T., Akinaga, S., Tamaoki, T. & Okabe, M. (1998). *Anticancer Drugs*, **9**, 653–657.
Kantarjian, H., Gandhi, V., Cortes, J., Verstovsek, S., Du, M., Garcia-Manero, G., Giles, F., Faderl, S., O'Brien, S., Jeha, S., Davis, J., Shaked, Z., Craig, A., Keating, M., Plunkett, W. & Freireich, E. J. (2003). *Blood*, **102**, 2379–2386.
Keating, M. J., O'Brien, S., Lerner, S., Koller, C., Beran, M., Robertson, L. E., Freireich, E. J., Estey, E. & Kantarjian, H. (1998). *Blood*, **92**, 1165–1171.
Kierdaszuk, B. & Eriksson, S. (1990). *Biochemistry*, **29**, 4109–4114.
Kierdaszuk, B., Rigler, R. & Eriksson, S. (1993). *Biochemistry*, **32**, 699–707.
Kraulis, P. J. (1991). *J. Appl. Cryst.* **24**, 946–950.
Laskowski, R. A., MacArthur, M. W., Moss, D. S. & Thornton, J. M. (1993). *J. Appl. Cryst.* **26**, 283–291.
Liliemark, J., Albertioni, F., Hassan, M. & Juliusson, G. (1992). *J. Clin. Oncol.* **10**, 1514–1518.
Lotfi, K., Mansson, E., Spasokoukotskaja, T., Pettersson, B., Liliemark, J., Peterson, C., Eriksson, S. & Albertioni, F. (1999). *Clin. Cancer Res.* **5**, 2438–2444.
Merritt, E. A. & Murphy, M. E. P. (1994). *Acta Cryst.* D**50**, 869–873.
Mikita, T. & Beardsley, G. P. (1988). *Biochemistry*, **27**, 4698–4705.
Montgomery, J. A., Shortnacy-Fowler, A. T., Clayton, S. D., Riordan, J. M. & Secrist, J. A. III (1992). *J. Med. Chem.* **35**, 397–401.
Otwinowski, Z. & Minor, W. (1997). *Methods Enzymol.* **276**, 307–326.
Parker, W. B., Shaddix, S. C., Chang, C. H., White, E. L., Rose, L. M., Brockman, R. W., Shortnacy, A. T., Montgomery, J. A., Secrist, J. A. III & Bennett, L. L. Jr (1991). *Cancer Res.* **51**, 2386–2394.
Parker, W. B., Shaddix, S. C., Rose, L. M., Shewach, D. S., Hertel, L. W., Secrist, J. A. III, Montgomery, J. A. & Bennett, L. L. Jr (1999). *Mol. Pharmacol.* **55**, 515–520.
Piro, L. D., Carrera, C. J., Beutler, E. & Carson, D. A. (1988). *Blood*, **72**, 1069–1073.
Pui, C. H., Jeha, S. & Kirkpatrick, P. (2005). *Nature Rev. Drug. Discov.* **4**, 369–370.
Reichelova, V., Liliemark, J. & Albertioni, F. (1995). *J. Pharm. Biomed. Anal.* **13**, 711–714.
Sabini, E., Ort, S., Monnerjahn, C., Konrad, M. & Lavie, A. (2003). *Nature Struct. Biol.* **10**, 513–519.
Santana, V. M., Mirro, J. Jr, Kearns, C., Schell, M. J., Crom, W. & Blakley, R. L. (1992). *J. Clin. Oncol.* **10**, 364–370.
Schüttelkopf, A. W. & van Aalten, D. M. F. (2004). *Acta Cryst.* D**60**, 1355–1363.
Sjöberg, A. H., Wang, L. & Eriksson, S. (1998). *Mol. Pharmacol.* **53**, 270–273.
Sorscher, E. J., Peng, S., Bebok, Z., Allan, P. W., Bennett, L. L. Jr & Parker, W. B. (1994). *Gene Ther.* **1**, 233–238.
Struck, R. F., Shortnacy, A. T., Kirk, M. C., Thorpe, M. C., Brockman, R. W., Hill, D. L., El Dareer, S. M. & Montgomery, J. A. (1982). *Biochem. Pharmacol.* **31**, 1975–1978.
Wang, L., Hellman, U. & Eriksson, S. (1996). *FEBS Lett.* **390**, 39–43.
Wang, L., Karlsson, A., Arner, E. S. & Eriksson, S. (1993). *J. Biol. Chem.* **268**, 22847–22852.
Warrell, R. P. Jr & Berman, E. (1986). *J. Clin. Oncol.* **4**, 74–79.
Wild, K., Bohner, T., Folkers, G. & Schulz, G. E. (1997). *Protein Sci.* **6**, 2097–2106.
Xie, C. & Plunkett, W. (1995). *Cancer Res.* **55**, 2847–2852.
Xie, K. C. & Plunkett, W. (1996). *Cancer Res.* **56**, 3030–3037.
Yamauchi, T., Nowak, B. J., Keating, M. J. & Plunkett, W. (2001). *Clin. Cancer Res.* **7**, 3580–3589.